J Med Sci 2016;36(4):145-151
DOI: 10.4103/1011-4564.188899

ORIGINAL ARTICLE

In Vitro Antibacterial and Anticancer Activity of Copper Oxide Nanostructures in Human Breast Cancer Michigan Cancer Foundation-7 Cells

J. Emima Jeronsia[1], D. J. Vidhya Raj[1], L. Allwin Joseph[1], K. Rubini[1], S. Jerome Das[1]

[1]*Department of Physics, Loyola College, Chennai, Tamil Nadu, India*

Objective: The use of nanoparticles (NPs) in cancer diagnosis and treatment is a rapidly developing area of nanotechnology. The main objective of this research work is to synthesize copper oxide (CuO) NPs and to investigate its vitro anticancer and antibacterial property. **Methods:** The CuO NPs were synthesized via a facile and cost-effective precipitation method using cupric acetate (monohydrate) ($CuAc_2.2H_2O$), sodium hydroxide, and glacial acetic acid. By varying the pH of the precursor solution, the morphology, particle size, and reaction rate of the NPs could be well tailored. The prepared CuO NPs were characterized by X-ray diffraction, ultraviolet-visible spectroscopy, Fourier transform infrared analysis, and scanning electron microscopy. **Results:** The results revealed a well crystalline structure with leaf-like morphology. By controlling the pH of the solution, particle size and morphology of the NPs are altered. The synthesized CuO NPs have been screened for its antibacterial potency against Gram-positive (*Methicillin-resistant Staphylococcus aureus* and *Bacillus subtilis*) and Gram-negative (*Salmonella Paratyphi*, *Klebsiella pneumonia*, and *Enterobacter aerogenes*) bacterial strains. The as-synthesized NPs were found to be remarkable in inhibiting pathogenic bacteria. The anticancer activity reveals the dose-dependent influence of CuO NPs against human breast cancer cell line Michigan Cancer Foundation-7 (MCF-7). **Conclusions:** The results suggested that CuO NPs have a wide range of antibacterial applications which can be used to control the spread and infection of a variety of bacterial strains. The CuO NPs showed promising anticancer activity against human breast cancer cell line (MCF-7). Overall, CuO NPs are an effective candidate for pharmaceutical, biomedical, and environmental applications.

Key words: Copper oxide, precipitation method, antibacterial efficacy, anticancer activity

INTRODUCTION

Cancer is a key cause for the leading mortality rate, among other scourges of humanity, which requires immediate intervention. Nowadays, breast cancer persists to be the most important cause of death globally.[1] According to the reports available, the use of existing chemotherapy drugs has their disadvantages such as high cost, perniciousness, and severe side effects. It is essential to discover alternative therapies, nanodrugs, and nanoformulations for drug delivery to conquer the situation. The proper combination of nanomaterials and biology will not only toughen the fight against pathogenic microorganism but can also render an outcome toward combating infectious diseases.[2]

In the broad-spectrum of biologically active nanoparticles (NPs), metal NPs such as Ag, Au, and Cu are the most sought after nanomaterials and increasingly used in medical and consumer products because of their high surface to volume ratio with small dimension.[3-10] Latterly, metal oxide NPs as an antimicrobial and anticancer agent has drawn considerable interest as a result of their unprecedented performance, enhanced properties, life cycle cost, and uniquely large applicability in various industrial fields and biomedical applications. Despite the great progress in nanotechnologies, to date, there is still a lack of definite knowledge on the effects of copper oxide (CuO) NPs on cancer cell lines. The previous history of NPs research shows that they seem to have

Received: November 30, 2015; Revised: February 04, 2016; Accepted: July 19, 2016

Corresponding Author: Dr. S. Jerome Das, Department of Physics, Loyola College, Chennai - 600 034, Tamil Nadu, India. Tel: +91-44-28178200; Fax: +91-44-28175566. E-mail: jeroemi@gmail.com

How to cite this article: Jeronsia JE, Vidhya Raj DJ, Joseph LA, Rubini K, Das SJ. *In vitro* antibacterial and anticancer activity of copper oxide nanostructures in human breast cancer Michigan Cancer Foundation-7 cells. J Med Sci 2016;36:145-51.

relative toxicity to cancer cells, without affecting the healthy cells. Noteworthy attention is directed toward CuO NPs as it is approximately 10-fold cheaper than silver and gold in the market and therefore, a method utilizing CuO would prove to be quite cost-effective. Moreover, CuO NPs have been investigated as antibacterial agent both against Gram-negative and Gram-positive microorganism and have high sensitivity even in the low concentration of CuO NPs; it is of special interest to view CuO NPs as anticancer agent, as well as an inorganic disinfectant.[11-17]

CuO is a p-type semiconductor with a narrow band gap (1.2 eV) and has been subjected to extensive investigations for its prospective applications in various fields such as gas sensors, catalysis, batteries, high-temperature superconductors, solar energy conversion, photovoltaic devices and field emission emitters.[18-22] Different methods have been proposed to synthesize CuO NPs such as hydrothermal synthesis,[23] sonochemical synthesis,[24] sol-gel method,[25] thermal decomposition,[26] colloidal thermal synthesis,[27] microwave irradiation,[28] thermal decomposition,[29] solution method,[30] and quick precipitation method.[31-34] Among these methods, hydrothermal and quick-precipitation methods have significance in safety and eco-friendly nature. Quick-precipitation is especially more attractive because of its fast, convenient, ease of mass production, cost-effectiveness, and environmentally friendly path to produce CuO NPs.

In this present work, CuO NPs with varying pH were synthesized by precipitation method to better understand the influence of pH for their applicability in increasing antibacterial activity against Gram-positive (*Methicillin-resistant Staphylococcus aureus* and *Bacillus subtilis*) and Gram-negative (*Salmonella Paratyphi*, *Klebsiella pneumonia*, and *Enterobacter aerogenes*) bacterial strains. Cytocompatibility of the synthesized CuO NPs was investigated against human breast cancer cell line Michigan Cancer Foundation-7 (MCF-7). Indeed, the results reveal conclusive evidence of the cytotoxic effect of CuO NPs against the MCF-7 cancer cell line.

MATERIALS AND METHODS

Materials

The starting materials used in this work were cupric acetate (monohydrate) ($CuAc_2.2H_2O$), sodium hydroxide, and glacial acetic acid obtained from Merck, India. All the chemicals were of analytical grade reagents commercially available and used without further purification. Double distilled water was used for the preparation of all aqueous solutions.

Preparation of copper oxide nanoparticles

A typical synthesis of CuO NPs was carried out as follows: 0.1 mol/L of cupric acetate and 0.2 mol/L of glacial acetic acid were dissolved in 50 ml of double distilled water. The effect of pH on NPs synthesis was determined by adjusting the pH of the reaction mixtures to 9, 10, 11, and 12. The solutions were stirred vigorously at room temperature for 3 h. The formation of CuO NPs was visually confirmed by the color change from green solution into a black precipitate. The process of centrifugation in the double distilled water was repeated thrice to ensure better separation of free entities from the solution. The obtained precipitate was placed in an oven at 60°C for 12 h and calcined at 200°C for 3 h and subsequently, the product was crushed into fine powder. The powdered CuO NPs were subjected to further studies.

Analysis of copper oxide nanoparticles

Preliminary characterization of CuO NPs was carried out using ultraviolet-visible (UV-Vis) spectroscopy; the measurement was done by Perkin Elmer Lambda 25 UV-Vis spectrometer from 200 to 800 nm. The Chou NPs synthesized by maintaining a solution pH of 12 was mixed with KBr and converted into pellet form by using bench process. Thereafter, the formed pellet was used to test for the functional groups by Fourier transform infrared analysis (FTIR) spectroscopy; the spectrum was recorded between 4000 and 400 cm^{-1}. The X-ray diffraction (XRD) spectra were recorded on Rich Seifert diffractometer using monochromatic CuK_α (λ =1.5406 Å) radiation. The data were collected in the 2θ range from 10 to 80° by using CuO powder. The morphology of the CuO NPs was visualized using a scanning electron microscope (SEM) without sputter coating because the NPs were self-conducting.

Antibacterial activity

The antibacterial activity of the synthesized CuO NPs was determined using the disc diffusion assay method. All glassware, media, and reagents used were sterilized in an autoclave at 121°C for 15 min. *Methicillin-resistant S. aureus* (Gram-positive), *S. aureus* (Gram-positive), *B. subtilis* (Gram-positive), *Salmonella Paratyphi* (Gram-negative), *K. pneumonia* (Gram-negative), and *E. aerogenes* (Gram-negative) were used as model test strains for both gram classes bacteria. Microbes were swabbed by means of cotton. Paper discs of 6 mm dimension were inserted with different amounts (1.25, 2.5 and 5 mg/ml) of CuO NPs. The plates were then incubated at 37°C for 24 h, and they were examined for the evidence of zones of inhibition, which appear as a clear area around the discs. The diameter of the clearing zones was measured in mm using the ruler scale.

Cell culture

MCF-7 human breast cancer cell lines were obtained from the National Centre for Cell Science, Pune, India. The cells were maintained in minimal essential medium supplemented with 10% fetal bovine serum, penicillin (100 U/ml), and streptomycin (100 μg/ml) in a humidified atmosphere of 50 μg/ml CO_2 at 37°C (Hi Media Laboratories, Mumbai, India). All of other chemicals and reagents were obtained from Sigma–Aldrich.

Dimethyl thiazolyl tetrazolium bromide assay

Dimethyl thiazolyl tetrazolium bromide (MTT) assay was performed to evaluate the cell viability and the inhibitory concentration (IC_{50}). Cells (1×10^5/well) was plated in 96-well plates and incubated for 24 h at 37°C in a humidified atmosphere of 95% air and 5% CO_2. After the human breast cancer cell, MCF-7 cells reach the confluence they were treated with a series of 10–500 μg/ml concentration of CuO NPs. A volume of 100 μl/well MTT was added to the cultures and incubated for 4 h and then 1 ml of dimethyl sulfoxide (DMSO) was added to all the wells. The absorbance at 570–620 nm was measured using UV-spectrophotometer with DMSO as blank. Measurements were performed, and the concentration required for a 50% inhibition (IC_{50}) has been determined graphically.

RESULTS AND DISCUSSION

X-ray diffraction pattern analysis

The XRD patterns of as-prepared CuO powders obtained at different pH values are depicted in Figure 1. The diffraction peaks of all samples were indexed, and it is found that the samples belonging to the monoclinic crystal system with lattice constants in Å as a = 4.662, b = 3.416, c = 5.118, and β = 99.49°. The diffraction peaks match with JCPDS file number 652309. The patterns explain a high purity of the samples since no additional peaks were present. The particle sizes were estimated from Scherrer formula: $D = 0.9\ \lambda/\beta \cos\theta$.

Where D is the average grain size, λ is the wavelength of X-ray, θ and β are the diffraction angle and full width at half maximum of the corresponding peaks. The diffraction peaks of the NPs were significantly broadened owing to the finite NPs size. Sharper CuO diffraction peaks were observed when the pH was maintained at 12. It is ascertained that the particle size can be varied as a function of pH of the medium [Figure 2].

Ultraviolet-visible spectrum

The UV-Vis diffuse reflectance spectrum of CuO nanostructures grown at different pH is shown in Figure 3. The spectra of all samples exhibit a single absorption

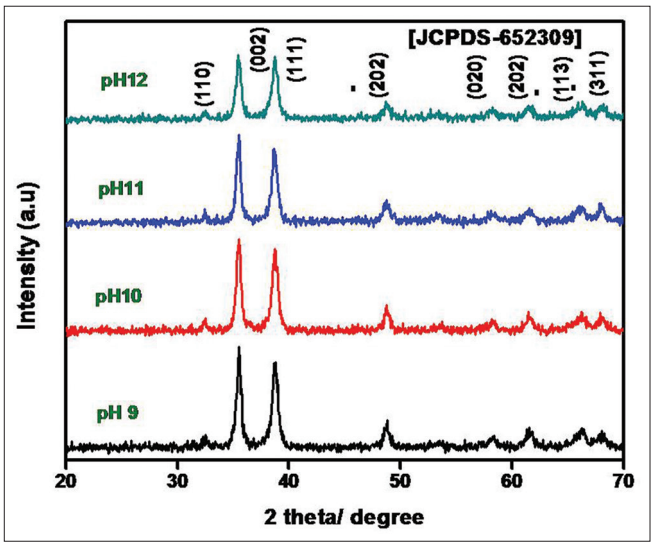

Figure 1: X-ray diffraction pattern of copper oxide nanoparticles at different pH

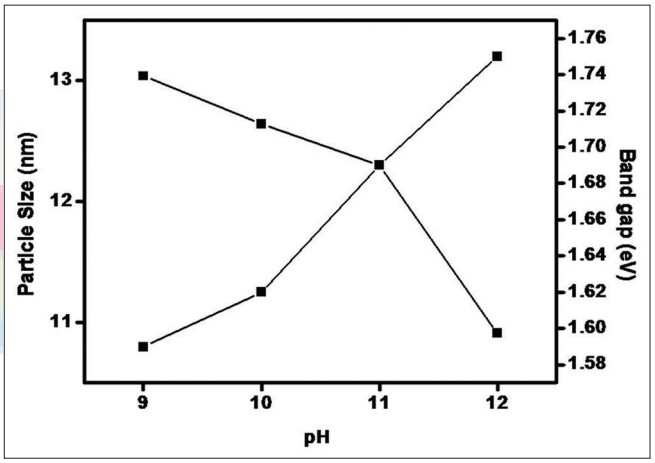

Figure 2: pH versus particle size and band gap

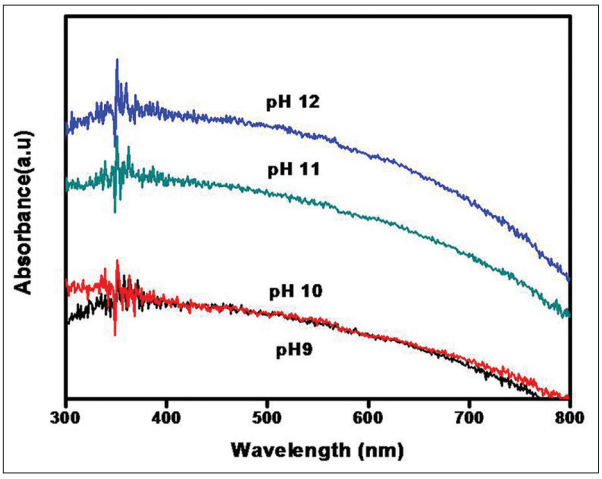

Figure 3: Ultraviolet-visible spectra of copper oxide nanoparticles at different pH

band centered at about 383 nm. According to the equation $\alpha Ep = A (Ep - Eg)^{½}$ (where α is the absorption coefficient, Ep is the discrete photon energy, Eg is the band gap energy, and A is a constant), the band gap in eV is calculated to be 1.59, 1.62, 1.69, and 1.75 which are higher than bulk CuO (Eg = 1.4 eV).[14] The blue shift behavior of the peak position is observed for the samples formed with the increase of pH due to their changing morphologies, particle size, and surface structure.

Fourier transform infrared analysis

FTIR analysis was performed to characterize the surface nature of the resulting CuO NPs, depicted as wavenumber versus transmittance in Figure 4. A strong absorption band at 532 cm^{-1} related to the vibrations of the CuO functional group. This confirmed the presence of nano-sized CuO particles. An intense and broadband contour which appears in the range of 3200–3550 cm^{-1} corresponds to the stretching mode of the hydroxyls of adsorbed water. Peaks appeared at 1410 and 1564 cm^{-1} corresponding to the C-O stretching of carboxylate ion bond to the CuO NPs as a bidentate ligand. The peak at 1564 cm^{-1} also represented the formation of a covalent bond between the – OH on the surface of CuO. A similar behavior was also observed by *A. El-Trass et al.*, *2012.*

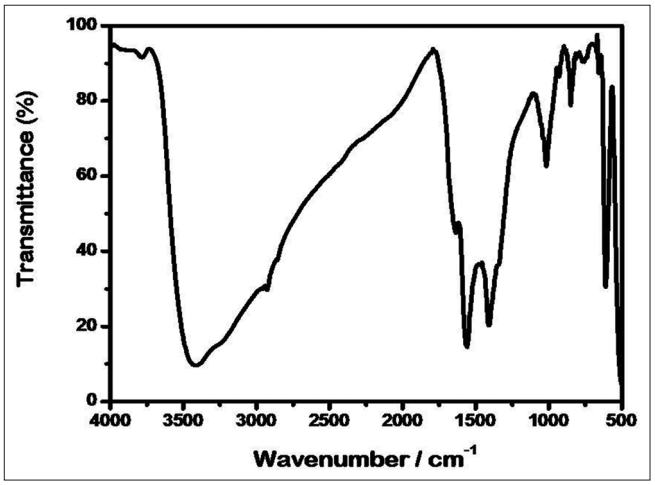

Figure 4: Fourier transform infrared spectrum of copper oxide nanoparticles

Scanning electron microscope analysis

Typical SEM images of CuO nanostructures prepared at different pH are shown in Figure 5. It reveals, there is a systematic evolution of different morphologies with an increase in pH [Figure 5a]. Shows a leaf-like morphology. The width of the leaf decreases as the pH increased. At pH 11, the leaf-like morphology is completely destroyed [Figure 5c] and only needle-like morphology exist when pH of the solution is 12 [Figure 5d]. These results show that the starting pH could not have much effect on the size and shape of the CuO NPs, whereas an increase in pH value could contribute to the formation of needle-shaped CuO NPs. Thus, the increase in pH results in the control of CuO NPs morphology.

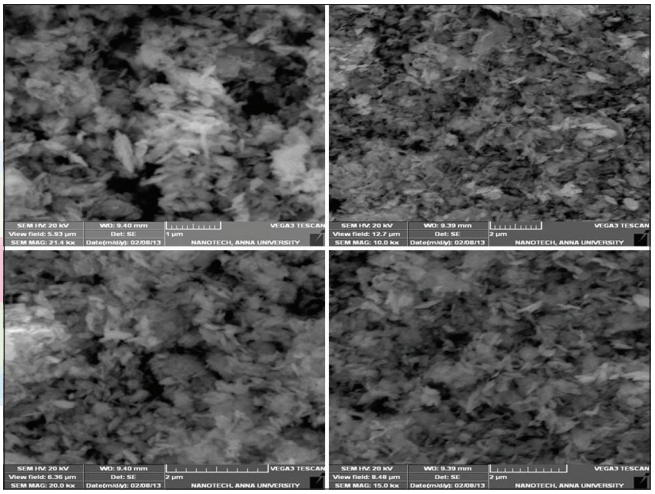

Figure 5: Scanning electron microscope images of copper oxide nanostructures at different pH (a) 9 (b) 10 (c) 11 (d) 12

Antibacterial performance

The antibacterial activity test results of CuO NPs against different Gram-positive (*Methicillin-resistant S. aureus, B. subtilis*) and Gram-negative (*Salmonella Paratyphi*, *K. pneumonia*, *E. aerogenes*) bacterial strains are shown in Figure 6.

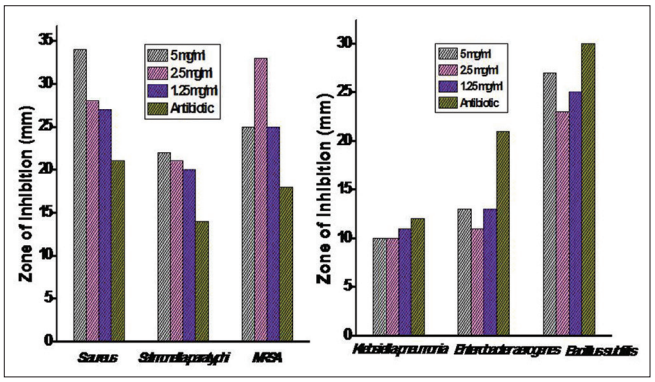

Figure 6: Disc diffusion assay for copper oxide nanostructures against bacterial strains

In the current study, CuO nanostructures with pH 12 alone displayed antibacterial activity against tested strains and the results were given in Table 1. A higher inhibition zone of 34 mm was observed in the Gram-positive *S. aureus* compared to other Gram-negative strains employed in this antibacterial susceptibility assay. For all bacterial strains, the highest activity was observed for 5 mg/ml but in the case of Gram-positive

Methicillin-resistant S. aureus higher inhibition zone of 33 mm was observed for the 2.5 mg/ml. Gram-positive (*S. aureus*, *Methicillin-resistant S. aureus*, and *Bacillus subtili)* depicted highest sensitivity to NPs compared to other strains and was more adversely affected by the CuO NPs between the zones of inhibition observed in disc diffusion method. Based on these results, it can be concluded that the synthesized CuO NPs had a significant antibacterial action on both the gram classes of bacteria. The bactericidal effects observed in this study might have been influenced by the release of Cu^{2+} ions in solution. Copper ions released by the NPs may attach to the negatively charged cell wall and rupture it, thereby leading to cell death. The mechanism proposed by[35,36] the copper ion binds with DNA molecules and lead to disorders of the helical structure by cross-linking within and between the nucleic acid strands and also disrupt the biochemical process. Figure 6 shown above represents the antibacterial activities of CuO NPs in pathogenic bacterial strains. It is observed that the Gram-positive bacterial strains have higher sensitivity than Gram-negative since the zone of inhibition is large in the former compared with the later.

Table 1: Zone of inhibition of synthesized copper oxide nanoparticles against various pathogenic bacteria

S.No	Bacterial Strains	Zone of inhibition (mm)			
		1.25 µg/ml	2.5 µg/ml	5 µg/ml	Antibiotic (Ampicillin)
1	*S.aureus*	34	28	27	21
2	Salmonella paratyphi	22	21	20	14
3	MRSA	25	33	25	18
4	Klebsiella pneumonia	10	10	11	12
5	Enterobacter aerogenes	13	11	13	21
6	Bacillus subtilis	27	23	25	30

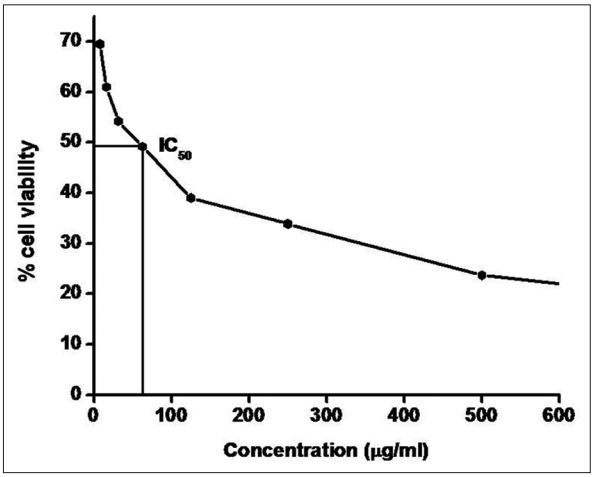

Figure 7: Percentage of viability on Michigan Cancer Foundation-7 cell lines

Cytotoxic activities of synthesized copper oxide nanoparticles against Michigan Cancer Foundation-7 cells

The as-synthesized CuO NPs have been tested for their potent cytotoxic activity against MCF-7 (breast cancer cells) using MTT assay. It is a sensitive colorimetric assay for the determination of the number of viable cells in cell proliferation and cytotoxicity assays. Figure 7 shows the proliferation rate, relative to nonexposed control cells, evaluated after 24 h and exposure to CuO NPs of various concentrations ranging from (10 µg/ml to 500 µg/ml). The result shows a decrease in proliferation rate with an increase in the concentration of CuO NPs. The half maximal inhibitory concentration (IC_{50}) was calculated as the concentration required to inhibit the growth of tumor cells in culture by 50% compared to the untreated cells. CuO NPs at the concentration of 62.5 µg/ml decreased the viability of MCF-7 cells by 50%.

The metabolic activity of MCF-7 cells presented a dose-dependent characteristic, which decreased with the decreasing of the dose of CuO NPs incubated with the MCF-7 cells. After 24 h of exposure, cell viability decreases as a result of mitochondrial dysfunction and the results suggest that CuO NPs were able to reduce the cell viability of MCF-7 cells in a dose-dependent mode. Figure 8 illustrates the images of MCF-7 cells exposed to CuO NPs. The quantification of cellular CuO NPs uptake using the imaging revealed a clear dose-dependent toxic activity. The morphological studies have shown, with the increasing CuO NPs concentration the MCF-7 cells were looking unhealthy and the cells were dying out of the population. The populations of MCF-7 cells were found to be more reduced at 125 µg/ml.

CONCLUSIONS

In summary, CuO NPs were proven to be a promising anticancer and antibacterial agent. The particle size and morphology of the NPs were controlled by varying the pH of the solution which improved the stability and significant

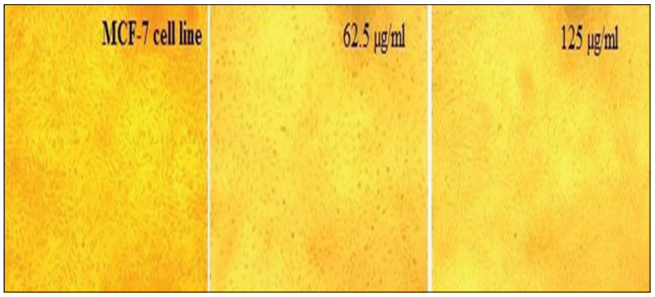

Figure 8: Toxic effect of synthesized copper oxide nanoparticles on Michigan Cancer Foundation-7 cell line

antibacterial activity of bacteria. It was confirmed that the survivability of bacteria decreases with the appending of proficient CuO NPs. Thus, the as-synthesized CuO NPs proved the outstanding antibacterial efficacy, and it was well established by the clear zone of inhibitions against bacterial strains. To this end, the cytotoxic effect of CuO NPs against human breast cancer cell line (MCF-7) was remarkable with 50% mortality at 62.5 μg/ml. Therefore, CuO NPs can be a promising candidate for pharmaceutical, biomedical, and environmental applications.

Financial support and sponsorship

This study was supported by the Loyola College, Chennai, Tamil Nadu, India.

Conflicts of interest

There are no conflicts of interest.

REFERENCES

1. National Cancer Institute, Breast Cancer Treatment; 2007. Available from: http://www.cancer.gov.
2. Boca SC, Potara M, Gabudean AM, Juhem A, Baldeck PL, Astilean S. Chitosan-coated triangular silver nanoparticles as a novel class of biocompatible, highly effective photothermal transducers for *in vitro* cancer cell therapy. Cancer Lett 2011;311:131-40.
3. Jeyaraj M, Sathishkumar G, Sivanandhan G, MubarakAli D, Rajesh M, Arun R, *et al.* Biogenic silver nanoparticles for cancer treatment: An experimental report. Colloids Surf B Biointerfaces 2013;106:86-92.
4. Lellouche J, Friedman A, Lellouche JP, Gedanken A, Banin E. Improved antibacterial and antibiofilm activity of magnesium fluoride nanoparticles obtained by water-based ultrasound chemistry. Nanomedicine 2012;8:702-11.
5. Dallas P, Sharma VK, Zboril R. Silver polymeric nanocomposites as advanced antimicrobial agents: Classification, synthetic paths, applications, and perspectives. Adv Colloid Interface Sci 2011;166:119-35.
6. Sharma VK, Yngard RA, Lin Y. Silver nanoparticles: Green synthesis and their antimicrobial activities. Adv Colloid Interface Sci 2009;145:83-96.
7. Prakash P, Gnanaprakasam P, Emmanuel R, Arokiyaraj S, Saravanan M. Green synthesis of silver nanoparticles from leaf extract of *Mimusops elengi*, Linn. for enhanced antibacterial activity against multi drug resistant clinical isolates. Colloids Surf B Biointerfaces 2013;108:255-9.
8. Ramyadevi J, Jeyasubramanian K, Marikani A, Rajakumar G, Rahuman AA. Synthesis and antimicrobial activity of copper nanoparticles. Mater Lett 2012;71:114-6.
9. Kora AJ, Sashidhar RB, Arunachalama J. Gum kondagogu (*Cochlospermum* gossypium): A template for the green synthesis and stabilization of silver nanoparticles with antibacterial application. Carbohydr Polym 2010;82:670-9.
10. Jagtap UB, Bapat VA. Green synthesis of silver nanoparticles using *Artocarpus heterophyllus* Lam. Seed extract and its antibacterial activity. Ind Crops Prod 2013;46:132-7.
11. Rao GN, Yao YD, Chen JW. Evolution of size, morphology, and magnetic properties of CuO nanoparticles by thermal annealing. J Appl Phys 2009;105:093-901.
12. Akhavan O, Ghaderi E. Cu and CuO nanoparticles immobilized by silica thin films as antibacterial materials and photocatalysts. Surf Coat Technol 2010;205:219-23.
13. Ren G, Hu D, Cheng EW, Vargas-Reus MA, Reip P, Allaker RP. Characterisation of copper oxide nanoparticles for antimicrobial applications. Int J Antimicrob Agents 2009;33:587-90.
14. Perelshtein L, Applerot G, Perkas N, Wehrschuetz-Sigl E, Hasmann A, Guebitz G, *et al*. CuO–cotton nanocomposite: Formation, morphology, and antibacterial activity.Surface & Coatings Technology 2009;204:54-7.
15. Baek YW, An YJ. Microbial toxicity of metal oxide nanoparticles (CuO, NiO, ZnO, and Sb2O3) to *Escherichia coli*, *Bacillus subtilis*, and *Streptococcus aureus*. Sci Total Environ 2011;409:1603-8.
16. Das D, Nath BC, Phukon P, Dolui SK. Synthesis and evaluation of antioxidant and antibacterial behavior of CuO nanoparticles. Colloids Surf B Biointerfaces 2013;101:430-3.
17. Xia J, Li H, Luo Z, Wang K, Yin S, Tenga F, *et al*. Sensors and Actuators B 2008;134:761-8.
18. Gao M, Sun L, Wang Z, Zhao Y. Controlled synthesis of Ag nanoparticles with different morphologies and their antibacterial properties. Mater Sci Eng C Mater Biol Appl 2013;33:397-404.
19. Reddy S, Kumara Swamy BE, Jayadevappa H. CuO nanoparticle sensor for the electrochemical determination of dopamine. Electrochim Acta 2012;61:78-86.
20. Suramwar NV, Thakare SR, Karade NN, Khatya NT. Green synthesis of predominant (1 1 1) facet CuO nanoparticles: Heterogeneous and recyclable catalyst for N-arylation of indoles. J Mol Catal A Chem 2010;359:28-34.
21. Wang SL, Li PG, Zhu HW, Tang WH. Controllable synthesis and photocatalytic property of uniform CuO/Cu_2O composite hollow microspheres. Powder Technol 2012;230:48-53.

22. Elfadill NG, Hashim MR, Chahrour KM, Qaeed MA, Bououdina M. The influence of Cu_2O crystal structure on the Cu_2O/ZnO heterojunction photovoltaic performance. Superlattices Microstruct 2015;85:908-17.
23. Jiang T, Wang Y, Meng D, Yu M. Facile synthesis and sssphotocatalytic performance of self-assembly CuO microspheres. Superlattices Microstruct 2015;85:1-6.
24. Tenga F, Yao W, Zhenga Y, Mac Y, Teng Y, Xu T, *et al*. Synthesis of flower-like CuO nanostructures as a sensitive sensor for catalysis. Sens Actuators B 2008;134:761-8.
25. Anandan S, Lee GJ, Wu JJ. Sonochemical synthesis of CuO nanostructures with different morphology. Ultrason Sonochem 2012;19:682-6.
26. Karthik K, Jaya NV, Kanagaraj M, Arumugam S. Temperature-dependent magnetic anomalies of CuO nanoparticles. Solid State Commun 2011;151:564-8.
27. Kong M, Zhang W, Yang Z, Weng S, Chen Z. Facile synthesis of CuO hollow nanospheres assembled by nanoparticles and their electrochemical performance. Appl Surf Sci 2011;258:1317-21.
28. Son DI, You CH, Kim TW. Structural, optical, and electronic properties of colloidal CuO nanoparticles formed by using a colloid-thermal synthesis process. Appl Surf Sci 2009;255:8794-7.
29. Guo L, Tong F, Liu H, Yan H, Li J. Shape-controlled synthesis of self-assembly cubic CuO nanostructures by microwave. Mater Lett 2012;71:32-5.
30. Hosny NM, Zoromba MS. Polymethacrylic acid as a new precursor of CuO nanoparticles. J Mol Struct 2012;1027:128-32.
31. Liu X, Li Z, Zhang Q, Li F, Kong T. CuO nanowires prepared via a facile solution route and their photocatalytic property. Mater Lett 2012;72:49-52.
32. Wua R, Maa Z, Gua Z, Yanga Y. Preparation and characterization of CuO nanoparticles with different morphology through a simple quick-precipitation method in DMAC-water mixed solvent. J Alloys Compd 2010;504:45-9.
33. Zhu J, Li D, Chen H, Yang X, Lu L, Wang X. Highly dispersed CuO nanoparticles prepared by a novel quick-precipitation method. Mater Lett 2004;58:3324-7.
34. Sahooli M, Sabbaghi S, Saboori R. Synthesis and characterization of mono sized CuO nanoparticles. Mater Lett 2012;81:169-72.
35. Azam A, Ahmed AS, Oves M, Khan MS, Habib SS, Memic A. Antimicrobial activity of metal oxide nanoparticles against gram-positive and gram-negative bacteria: A comparative study. Int J Nanomedicine 2012;7:6003-9.
36. Stohs SJ, Bagchi D. Oxidative mechanisms in the toxicity of metal ions. Free Radic Biol Med 1995;18:321-36.